ANALYSIS OF WATER USE EFFICIENCY USING ON-THE-GO SOIL SENSING AND A WIRELESS NETWORK

L. Pan, V.I. Adamchuk, D.L. Martin

Department of Biological Systems Engineering
University of Nebraska-Lincoln
Lincoln, Nebraska

M.A. Schroeder

Agricultural Research and Development Center
University of Nebraska-Lincoln
Mead, Nebraska

R.B. Ferguson

Department of Agronomy and Horticulture
University of Nebraska-Lincoln
Lincoln, Nebraska

ABSTRACT

An efficient irrigation system should meet the demands of crops. Though a limited water supply may result in yield reduction, excess irrigation is a waste of resources. To investigate water use efficiency, on-the-go sensing technology (in this case, field elevation and apparent electrical conductivity) has been used to reveal soil spatial variability relevant to water-holding capacity. These high-density data layers were used to identify strategic sites where monitoring water availability during the growing season allowed researchers to quantify shortages and/or excesses of water supply. Nine locations in a 37-ha agricultural field were selected for monitoring soil matric potential and temperature at four depths (18, 48, 78, and 108 cm) using wireless technology. These locations represent different growing conditions. The measurements were used to quantify the temporal variability of soil water content and water depletion, and then to assess whether optimization of the irrigation water supply could increase water use efficiency in comparison to the current practice of uniform irrigation scheduling.

Keywords: water use efficiency, on-the-go sensor, wireless network

INTRODUCTION

Shortages of available water resources and increases in energy costs motivate many producers to consider variable rate irrigation (VRI). The spatial variability of factors including topography, soil type, water availability, landscape features, and cropping systems results in differing demands for irrigated water. In response to this variability, VRI can be executed to improve water use efficiency, thereby increasing yield productivity, conserving fuel, and limiting fresh water consumption. VRI can also reduce nutrient leaching. An increasing number of research projects have focused on implementing VRI using two key technologies: (1) newly designed sprinkler systems capable of providing spatially varying irrigation rates and (2) software and hardware for control systems to guide VRI.

For example, King and Kincaid (2004) described laboratory testing which indicated that the variable flow rate sprinkler developed could potentially be used for VRI. In another research project, the operational equation that described the internal connection of the flow rate, rotating speed, and throw distance of the variable rate contour-controlled sprinkler was derived using the mathematical theory of limitation and double integral (Han et al., 2007). This provided fundamental principles for the design of variable rate contour-controlled sprinklers and square wetted area sprinklers.

In terms of controller development, the modern control panels provide center pivot operators with the potential to monitor and change center pivot operations using cellular or radio telemetry as well as by using the Internet or satellite communication (Kranz, 2009). Kim et al. (2006) reported on the development of a graphical user interface for wireless monitoring and control of sprinkler irrigators with VRI capabilities. Bao et al. (2004) integrated dielectric soil properties measurements, relevant data processing, fuzzy control arithmetic, a Global Positioning System (GPS) receiver, and virtual instrument systems to achieve VRI as well. Hedley et al. (2009) compared VRI and uniform rate irrigation (URI) and showed that VRI saved 9-19% of irrigation water, reduced the loss of drainage water by 25-45%, and reduced the risk of nitrogen leaching. Though the benefits of VRI are obvious, capable systems are rather expensive. However, as more producers adopt VRI systems, the cost of this technology will likely drop.

In addition to obtaining the key technologies aimed at the direct implementation of VRI, it is important to focus on defining the amount of irrigated water demand across the entire agricultural field. Conventional on-the-spot evaluation of soil conditions is somewhat subjective and labor-intensive. In addition, spatial soil variability within a field can be quite extensive, which means that defining representative locations to make irrigation management decisions is challenging.

By contrast, on-the-go soil sensing has been able to provide fine-resolution maps of soil properties at a relatively low cost (Adamchuk et al., 2004). Such instruments provide the capacity to map soil topography, apparent soil electrical conductivity (EC_a), optical reflectance, mechanical resistance, capacitance, and other properties. Unfortunately, the relationships between the data detected on-the-go and agronomic soil parameters, such as water content, are site-specific. In addition, the amount of water stored in soil profile changes not only spatially, but also temporally. Therefore, sensor-based maps have been used to define the

spatial variability of soil properties influencing water movement across a landscape, and this information has been used to define relatively homogeneous management zones that have been evaluated separately (Hedley, 2009).

Wireless technology has been used increasingly to achieve temporal monitoring of soil conditions. Such systems allow the producer to obtain information about soil matric potential, water content, temperature, and other properties in real time from a remote location (Kim et al., 2006). This greatly improves the convenience of monitoring soil water for the producer. The data have been used by irrigation systems managers to optimize the use of resources in response to dynamic changes in soil conditions and reduce the risk of crop water stress (Lamm and Aiken, 2008; Moore et al., 2005; Rodrigues et al., 2003).

The objective of this research is to optimize irrigation management (possibly recommending VRI) using both fine-resolution maps of EC_a and field elevation in combination with temporal monitoring of soil matric potential using a wireless sensor network.

MATERIALS AND METHODS

A 37-ha field (Field 1.14) at the Agricultural Research and Development Center (ARDC) near Mead, Nebraska was chosen as the field in which to explore the opportunity to optimize water use during irrigation season (Fig. 1). First the field was mapped using a Veris® 3150 unit (Mobile Sensor Platform, Veris Technologies, Inc., Salina, Kansas) equipped with an RTK-level AgGPS® 442 GNSS receiver (Trimble Navigation Ltd., Sunnyvale, California)[1]. Then, obtained maps of shallow (0-30 cm) EC_a and field elevation were used to determine nine field locations with differing expected water demands. Researchers installed nodes for a wireless sensor network monitoring soil matric potential and temperature at four depths (18, 48, 78, and 108 cm) in each of these nine locations. Spatially and temporarily changing water demand was defined using percent water depletion estimates that are normally expected to remain in the range between 30 and 50% throughout the entire crop-growing season.

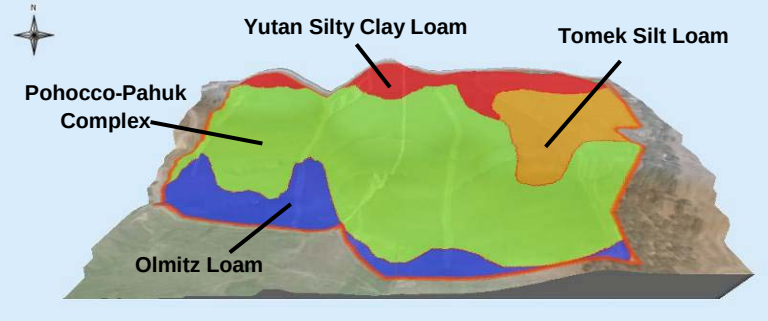

Fig. 1: Field 1.14 at the University of Nebraska-Lincoln Agricultural Research and Development Center (Mead, Nebraska).

[1] Mention of a trade name, proprietary product, or company name is for presentation clarity and does not imply endorsement by the authors or the University of Nebraska-Lincoln, nor does it imply exclusion of other products that may also be suitable.

Sensor Installation Locations

To define soil water content monitoring sites, EC_a and field elevation maps shown in Fig. 2 were analyzed using three combined optimization criteria (Adamchuk et al., 2009). These criteria included: (1) complete spatial field coverage using the S-optimality criterion; (2) even distributions throughout both data layers using the D-optimality criterion; and (3) the relative homogeneity of the selected sites using a criterion developed based on the sum of squared differences between measurements obtained in each location and its immediate neighbor locations. The overall objective function was the geometric mean of these criteria normalized against the median of a large number of random selections.

Fig. 2: Maps of topsoil EC_a and field elevation with selected sensor installation locations.

As a result, the same number of locations represented three physical parts of the field divided by two waterways, and the same number of locations represented areas with low and high ECa as well as low and high field elevations (Fig. 3). Also, the northeastern location (Node 9) represented a non-irrigated area when the northwestern location (Node 7) was covered by the end gun, the southeastern location (Node 3) was at the pivot stopping position, and the rest of nodes represented different distances from the center of the irrigation pivot system (Fig. 4).

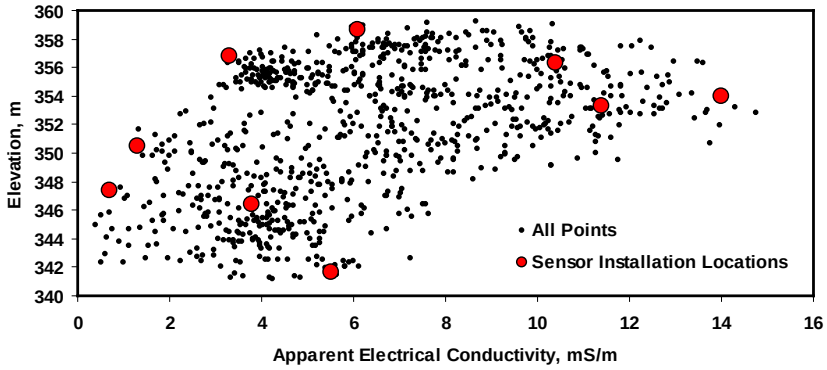

Fig. 3. Relationship between ECa and field elevation.

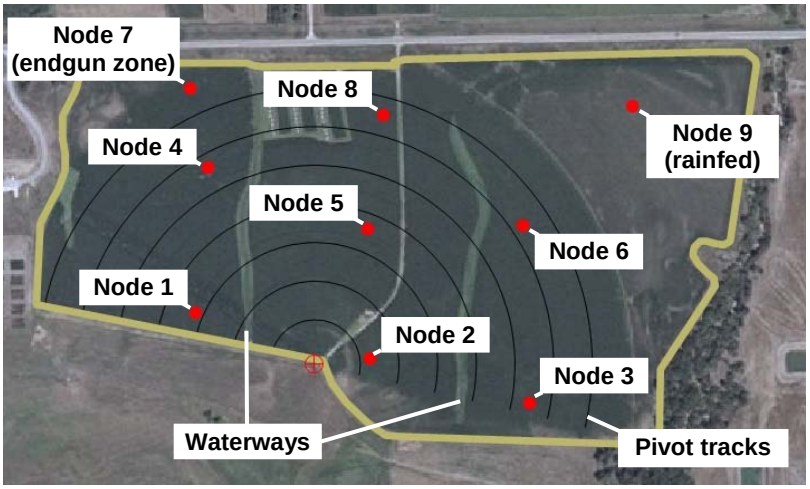

Fig. 4. Geometry of the center-pivot irrigation system with respect to the sensor locations selected.

Sensor Network Installation

As shown in Fig. 5, each monitoring location was established using a wireless communication node equipped with a solar panel and batteries to provide a continuous power supply (eN2100 eKo Node, Crossbow Technology, Inc., San Jose, California). Each sensor array was comprised of four thermistors and four soil matric potential sensors with their centers placed 18, 48, 78, and 108 cm below the surface. Each sensor was intended to represent a 1 ft (30 cm) layer of soil. The soil matric potential is related to the energy that must be available in plants to extract water stored in the soil profile. The electrical resistance type soil matric potential sensors were Watermark® Granular Matrix sensors with attached thermistors (eS1101, Crossbow Technology, Inc., San Jose, California). In such a sensor, electrical resistance between two electrodes imbedded in a sensor responds to water moved through new transmission material with a consistency close to that of fine sand. The sensors were calibrated at the temperature of 21°C. Measurements conducted using thermistors installed at the same depth were used to adjust soil matric potential measurements according to:

$$\psi_{adj} = \psi + 0.018(T - 21) \tag{1}$$

where Ψ_{adj} is the temperature-corrected soil matric potential (kPa); Ψ is the original soil matric potential measurement (kPa); and T is the soil temperature (°C). Both Ψ and Ψ_{adj} values are negative.

All the nodes were connected into a wireless sensor network (shown in Fig. 6) with a 2.4 GHz communication frequency. The eKo Gateway (eG2100, Crossbow Technology, Inc., San Jose, California) was installed in a nearby building to store the data sent by each node in 15 minute time intervals, as well as to view and manage data using the eKoView web interface. The eKo Base Radio (eB2110, Crossbow Technology, Inc., San Jose, California) had an added Omni-directional

antenna (HAO15SIP, Hawking Technology, Inc., Irvine, California) to ensure a reliable connection between the base and the nodes in the signal-covered area.

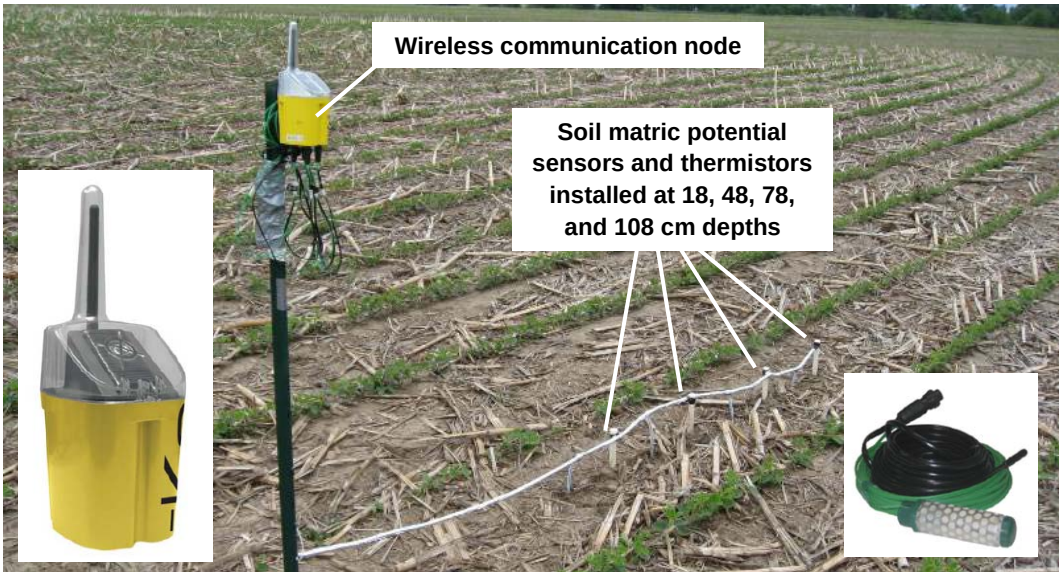

Fig. 5. Soil water content monitoring location.

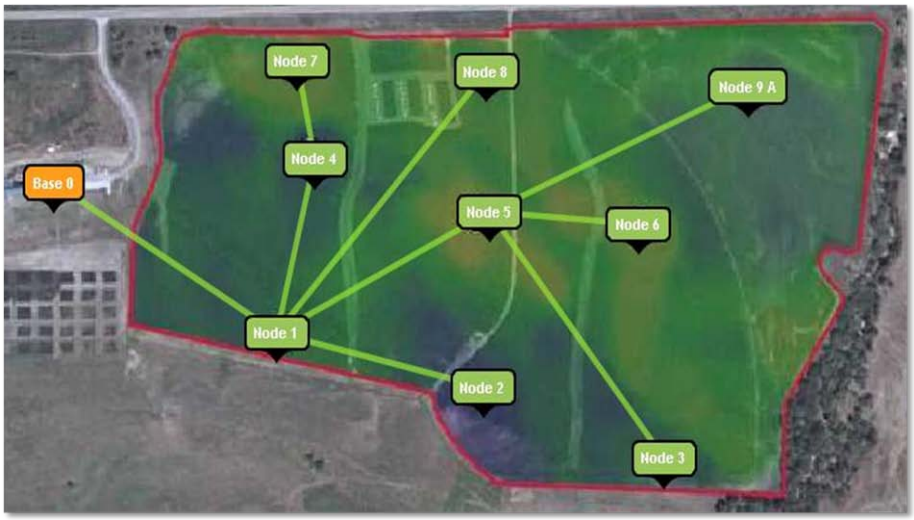

Fig. 6. The wireless sensor network.

In addition to the monitoring of soil matric potential and temperature, an additional node was installed at the edge of the field to monitor atmospheric conditions (Fig. 7). It was connected to an ambient temperature and humidity sensor (ES1201, Crossbow Technology, Inc., San Jose, California) and a tipping bucket rain gauge (TB3, Hydrological Services Pty. Ltd., Warwick Farm, New South Wales, Australia). An add-on sensor board (ES9200, Crossbow Technology, Inc., San Jose, California) was used as an interface between the rain gauge and the communication node.

During the 2009 growing season, the experimental field was used to produce soybeans. The irrigation schedule was followed as usual – according to soil

conditions around Node 8. Experimental data was collected from June 29 to October 4, which corresponds to the 14 week growing period with the highest water demand. Fig. 8 illustrates the weekly water supply (including both precipitation and irrigation). It appears that though the irrigation season started at the end of July, there was no need for irrigation after a few major rainfall events in the middle of August.

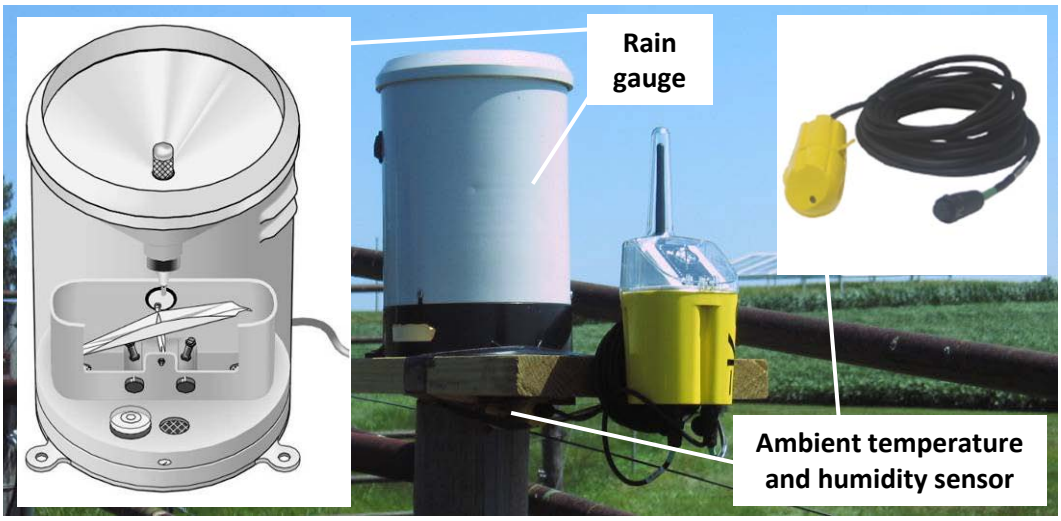

Fig. 7. Atmospheric conditions monitoring location.

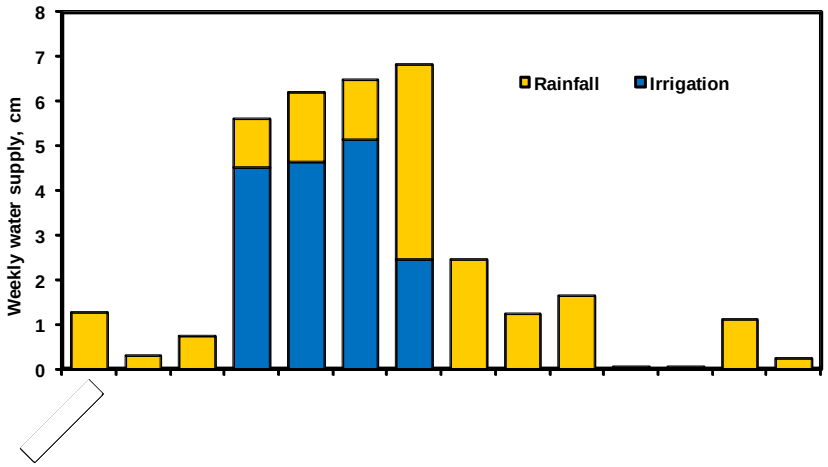

Fig. 8. Weekly water supply for the experimental site during the summer of 2009.

To accomplish the research objectives, data processing involved defining the time and duration of limited water availability in each of the monitoring locations and comparing the irrigation demand among selected sites representing diverse field conditions.

Data Interpretation

All the experimental data were stored in comma-delimited text files. Prior to data processing, all erroneous (e.g., loose sensor connection) measurements were removed from the dataset and temperature compensation was applied to soil

matric potential measurements. Some data were lost, in the majority of cases because of loose wire connections for certain sensors. After that, weekly averages were calculated to summarize soil water availability for the fourteen weeks covering the period of this study.

The Saxton 2005 model (Saxton and Rawls, 2005) was used to define the relationships between soil matric potential and volumetric water content in each location and depth based on soil texture and organic matter content analyzed in a commercial soils lab. Although soil texture was analyzed for each sensor placement, average organic matter content was determined only for the topmost soil layer around each monitoring location. Typical soil series profiles were used to estimate deeper values. The following equation was used:

$$\Psi_\theta = \mathbf{A}(\theta_V)^{-\mathbf{B}} \tag{2}$$

where Ψ_θ is the soil matric potential (kPa); A and B are location-specific coefficients; and θ_V is the soil volumetric water content (cm^3/cm^3).

The coefficients A and B were found to fit a linear relationship between $ln(\Psi_\theta)$ and $ln(\theta_V)$ using estimated volumetric water content at Ψ = 33 kPa and wilting point (Ψ = 1500 kPa). Corresponding estimates of θ_V were found based on percent clay, percent sand, and organic matter measurements according to Saxton and Rawls (2005).

From the known value of volumetric water content, percent depletion was calculated as a fraction of volumetric water content corresponding to field capacity:

$$Depletion = \frac{\theta_{fc} - \theta}{\theta_{fc} - \theta_{wp}} \cdot 100\% \tag{3}$$

where *Depletion* is percent depletion; θ_{fc} is the volumetric water content at field capacity (cm^3/cm^3); and θ_{wp} is the volumetric water content at wilting point (Ψ = 1500 kPa, cm^3/cm^3).

Based on the estimates of field capacity summarized by Melvin and Yonts (2009) for a variety of soil textures, volumetric water content and soil matric potential values at field capacity for each location were assumed, and volumetric water content values at wilting point (Ψ = 1500 kPa) were estimated according to Table. 1.

RESULTS AND DISCUSSION

The change of soil matric potential at each site for the duration of this study is summarized in Fig. 9. Measurements of Ψ_θ were relatively low in the beginning of the growing season (wet soil) with gradual drying until the middle of August when a substantial rainfall took place, after which the “drying out” process started again. Also, as one would expect, deeper soil layers dried slower than shallower soil layers.

Estimated soil volumetric water content (Fig. 10) also indicates higher temporal dynamics closer to the surface and greater water storage capacity deeper in the profile. Finally, percent depletion estimates (Fig. 11) indicated that based

on the accepted water retention curve, none of the field locations experienced severe water stress (percent depletion above 50%). Node 3 is located in sandy soil which contributed to relatively high values of soil matric potential near the soil surface. During sensor installation at Node 3, a compacted sand pan was discovered at approximately 70 cm below the soil surface which may have restricted root development and caused more extraction from the shallow depths and contributed to wetter soil deeper in the profile.

Table. 1. θ_V and Ψ at field capacity for each location based on soil textural classes.

Node	Depth, cm	Clay, %	Sand, %	Soil Texture Class	θ_V, cm^3/cm^3		Ψ, kPa
					Wilting point	Field capacity	
1	18	20	41	Loam	0.14	0.33	13.0
1	48	26	34	Loam	0.17	0.36	14.0
1	79	24	39	Loam	0.16	0.33	14.7
1	109	21	45	Loam	0.13	0.30	14.2
2	18	4	90	Sand	0.02	0.09	13.5
2	48	6	88	Sand	0.04	0.10	15.0
2	79	6	91	Sand	0.03	0.08	14.0
2	109	4	91	Sand	0.02	0.08	14.8
3	18	18	57	Sandy Loam	0.12	0.24	25.7
3	48	14	65	Sandy Loam	0.10	0.21	16.2
3	79	10	79	Sandy Loam	0.06	0.14	17.6
3	109	6	90	Sand	0.03	0.09	16.1
4	18	7	80	Loamy Sand	0.05	0.12	19.9
4	48	6	85	Loamy Sand	0.04	0.11	17.3
4	79	5	86	Loamy Sand	0.03	0.09	15.7
4	109	2	91	Sand	0.01	0.07	15.8
5	18	34	15	Silty Clay Loam	0.21	0.36	41.8
5	48	30	14	Silty Clay Loam	0.19	0.34	48.8
5	79	23	17	Silt Loam	0.15	0.31	38.7
5	109	15	15	Silt Loam	0.10	0.27	48.7
6	18	36	17	Silty Clay Loam	0.22	0.37	37.4
6	48	39	14	Silty Clay Loam	0.24	0.39	34.5
6	79	42	10	Silty Clay	0.25	0.38	46.6
6	109	29	22	Clay Loam	0.18	0.33	38.2
7	18	33	16	Silty Clay Loam	0.21	0.36	42.7
7	48	34	16	Silty Clay Loam	0.21	0.36	39.6
7	79	30	15	Silty Clay Loam	0.19	0.34	45.7
7	109	22	13	Silt Loam	0.14	0.31	44.5
8	18	27	20	Silt Loam	0.18	0.34	36.3
8	48	35	16	Silty Clay Loam	0.21	0.36	38.3
8	79	43	14	Silty Clay	0.26	0.39	41.3
8	109	33	14	Silty Clay Loam	0.20	0.35	41.9
9	18	25	16	Silt Loam	0.16	0.33	42.3
9	48	33	14	Silty Clay Loam	0.20	0.35	42.9
9	79	34	12	Silty Clay Loam	0.21	0.36	43.1
9	109	36	14	Silty Clay Loam	0.22	0.37	37.9

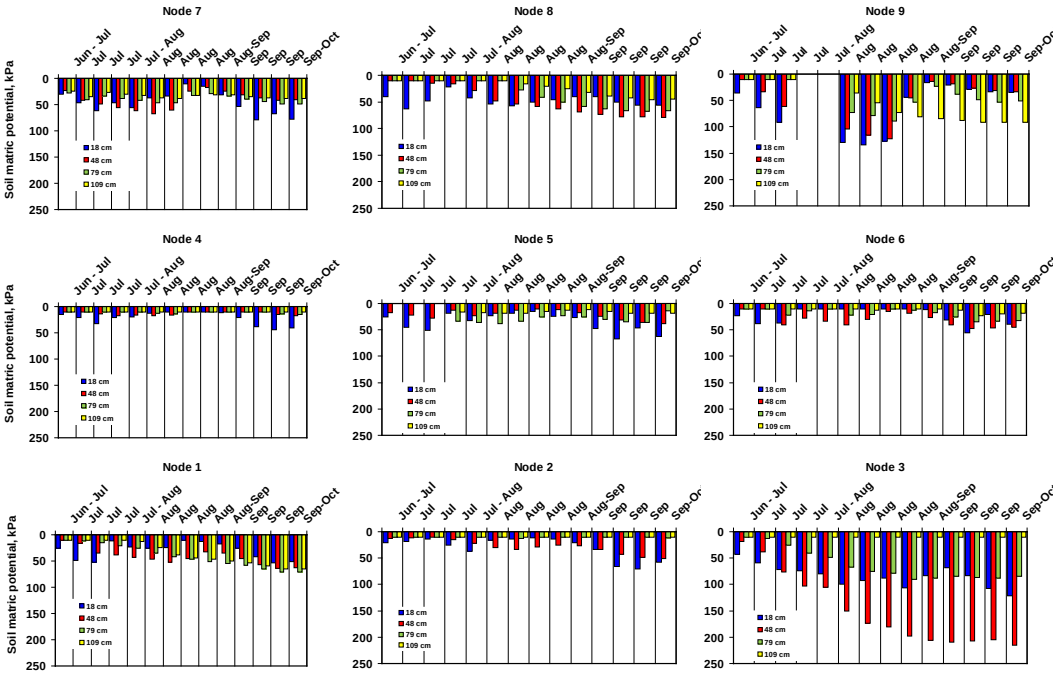

Fig. 9. Weekly average of soil water matric potential (kPa).

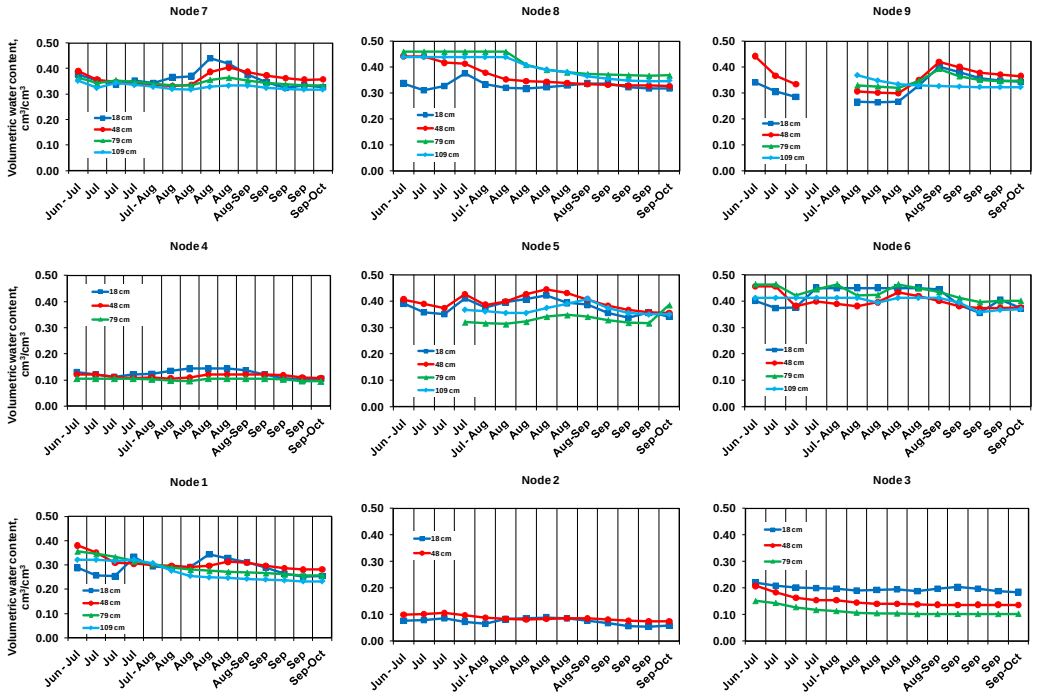

Fig. 10. Weekly average soil volumetric water content (cm^3/cm^3).

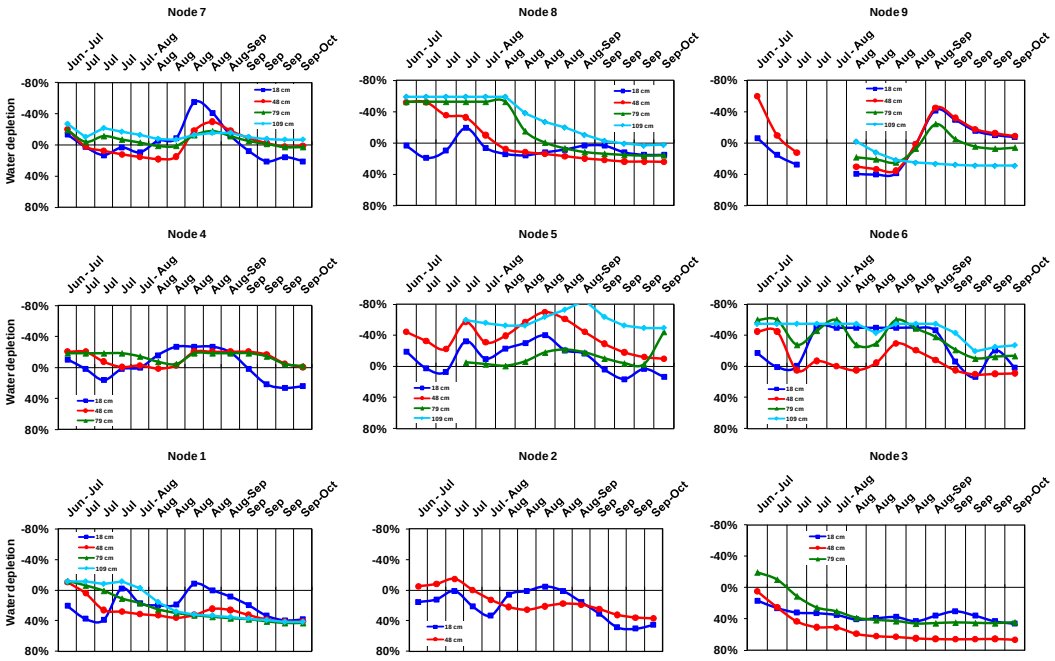

Fig. 11. Weekly average depletion for each depth at the measurement sites.

Generalizations are more apparent when evaluating the change of water depletion for whole soil profiles (Fig. 12). The profile depletion is the cumulative depletion for all soil layers relative to the water-holding capacity of the profile. Sandy soils at Node 3 dried to about 40% depletion by the middle of August. Other sandy Nodes (2 and 4) did not dry as extensively as Node 3. Soils at the rest of the irrigated nodes were finer textured, which allowed soil water depletions to remain below 30% most of the growing season. All of the soil water measurements indicate that throughout the 2009 growing season the water supply was sufficient to avoid water stress, partially due to the timely irrigation.

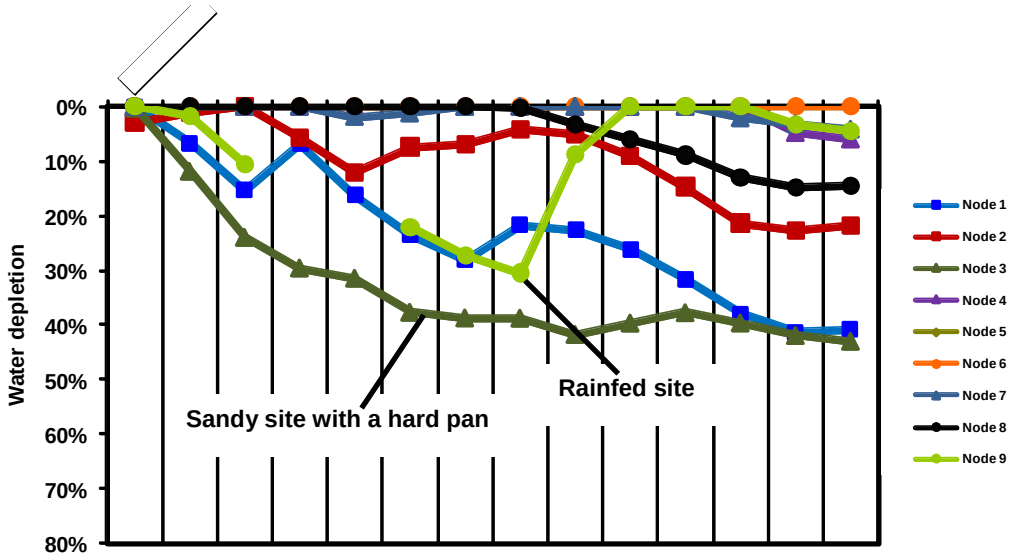

Fig. 12. Weekly average soil water depletion for the soil profile.

However, it is important to note that at Node 9 (a rainfed location with fine-textured soil) installed sensors did not exhibit a significant shortage of water during the growing season. Apparently, August rainfalls were sufficient to recharge the soil profile through the remainder of the growing season, which explains why irrigation was terminated early in the season. It appears that had precipitation been lower, severe depletion could have been reached near the end of August. The option to fine-tune irrigation scheduling to optimize water use will be investigated in 2010 when corn will be grown in the field.

CONCLUSIONS

In this research, the apparent soil electrical conductivity and field elevation maps were used to establish a wireless network of nine nodes to monitor soil matric potential and temperature at four depths throughout the growing season for soybeans grown in a 37-ha production field with a center pivot irrigation system. The network provided the capability of visualizing and storing data remotely. A soil water retention model combined with measured or assumed estimates of soil texture and organic matter content were used along with soil matric potential and soil temperature measurements to predict the volumetric water content and, ultimately, the depletion of available water throughout the growing season. Due to the sufficient level of precipitation during the summer 2009, significant water stress was not present and the need for variable rate irrigation management was not obvious. However, it was clear that coarse-textured soils located predominantly along the lower field elevations had water regimes that differed from the rest of the field. Further investigations will be conducted in the summer of 2010 when the same field will be planted in corn.

ACKNOWLEDGEMENT

This publication is a contribution of the University of Nebraska Agricultural Research Division, supported in part by funds provided through the Hatch Act and by funds provided through the Nebraska Center for Energy Science Research through the Water, Energy and Agriculture Initiative (WEAI).

REFERENCES

Adamchuk, V.I., Hummel, J.W., Morgan, M.T. and Upadhyaya, S.K. 2004. On-the-go soil sensors for precision agriculture. *Computer and Electronics in Agriculture* 44(1): 71-91.

Adamchuk, V.I., Pan, L., Marx, D.B., and Martin, D.L. 2009. Site-specific calibration of multiple soil sensor data layers. Paper No. 09-5782. ASABE, St. Joseph, MI.

Bao, Y., Wu, Y., He, Y., Wang, L. 2004. Study on signal processing for a crop irrigation virtual instrument system. ASAE Publication No. 701P1004. ASAE, St. Joseph, MI.

Han, W., Fen, H., Wu, P., Yang, Q. 2007. Variable-rate contour-controlled sprinklers for precision irrigation. Paper No. 072249. ASABE, St. Joseph, MI.

Hedley, C. 2009. A method for spatial prediction of daily soil water status for precise irrigation scheduling. *Agricultural Water Management* 96(12): 1737-1745.

Hedley, C., Yule, I., Tuohy, M., Vogeler, I. 2009. Key performance indicators for variable rate irrigation implementation on variable soils. Paper No. 096372. ASABE, St. Joseph, MI.

Kim, Y., Evans, R.G., Iversen, W., Pierce, R.J., Chavez, J.L. 2006. Software design for wireless in-field sensor-based irrigation management. Paper No. 063074. ASABE, St. Joseph, MI.

King, B.A., and Kincaid, D.C. 2004. A variable flow rate sprinkler for site-specific irrigation management. *Applied Engineering in Agriculture* 20(6): 765-770.

Kranz, W. 2009. Monitoring irrigation water application with computerized controllers. In: *Proceedings of the 21st Annual Central Plains Irrigation Conference*. CPIA, Colby, Kansas, pp. 201-206.

Lamm, F.R., and Aiken, R.M. 2008. Comparison of temperature-time threshold and ET-based irrigation scheduling for corn production. Paper No. 084202. ASABE, St. Joseph, MI.

Melvin, S.R., and Yonts, C.D. 2009. Irrigation scheduling: checkbook method. *EC709*. University of Nebraska-Lincoln Extension. Lincoln, NE.

Moore, S., Han, Y.J., Niyazi, B. 2005. Instrumentation for variable-rate lateral irrigation system. Paper No. 052184. ASABE, St. Joseph, MI.

Rodrigues, F., Yoder, R., Wilkerson, J. B. 2003. A site-specific irrigation control system. Paper No. 031129. ASABE, St. Joseph, MI.

Saxton, K.E. and Rawls, W.J. 2006. Soil water characteristic estimates by texture and organic matter for hydrologic solutions. *Soil Science Society of America Journal* 70: 1569-1578.